RESEARCH ARTICLE

Integrating machine learning and Monte Carlo Simulation for probabilistic assessment of durability in RC structures affected by carbonation-induced corrosion

Emerson F. Felix[1] · Breno M. Lavinicki[2] · Tobias L. G. T. Bueno[1] · Thiago C. C. de Castro[1] · Renan A. Cândido[1]

Abstract

This study introduces an original approach that integrates a machine-learning algorithm and a Monte Carlo simulation technique to evaluate the durability of reinforced concrete (RC) structures subjected to carbonation-induced corrosion. The study commences by forecasting the carbonation depth of concrete samples subjected to natural conditions, employing Artificial Neural Networks (ANNs) with the backpropagation algorithm. A database was created by gathering information from 870 literature sources, and it was utilized to build 100 ANN models with different topologies. A rigorous evaluation was conducted to identify the most efficient ANN architecture. Subsequently, the approach was applied in a case study to evaluate the design life of structures in a real scenario, thereby demonstrating its tangible value in real-world applications. In addition, a parametric study was undertaken to examine the material's compressive strength and the thickness of the concrete cover, which influences its durability. The design life was determined using the Monte Carlo Simulation technique coupled with the ANN model, in which the probability of depassivation due to carbonation was forecasted. Findings indicate that decreasing the concrete cover by 25% would lead to a 48% decrease in the structure's design life, highlighting the influence of accurately determining and implementing the thickness of the concrete cover for RC structures.

Keywords Concrete carbonation · Durability · Reinforcement depassivation · Machine learning

1 Introduction

Corrosion significantly decreases the lifespan of reinforced concrete structures. The World Corrosion Organization reports that the expenses of this destructive phenomenon surpass 3% of the Gross Domestic Product (GDP) in multiple nations. The prevalence of this deteriorative process in reinforced concrete structures is notable, with rates reaching up to 48% in South Africa, 25% in the United Kingdom, 36% in India, and 31% in the United States [1]. Corrosion rates in Brazil vary from 14 to 64% depending on the location being studied [2, 3].

Oxidation leads to reinforcement corrosion, creating an oxide coating around the metallic element. This corrosion type progresses slowly at room temperature (± 25 °C), unless exposed to severe conditions or highly aggressive gases like CO_2 and chloride ions in the atmosphere [4–6].

Carbonation-induced corrosion occurs uniformly over the longitudinal portion of the reinforcement due to CO_2 diffusion into the concrete matrix. The corrosive process happens at a regulated speed, influenced by numerous factors, either environmental or associated with material characteristics [7–9]. Key environmental factors are CO_2 concentration in the atmosphere, rainfall frequency, relative humidity, and temperature [6, 10–13]. Internal factors include the water-binder ratio used in concrete production, compressive strength, concrete cover thickness, and concrete composition [5, 14–18].

Andrade [3] categorizes corrosion degradation on RC structures as a decrease in mechanical capacity, weakening

✉ Emerson F. Felix
emerson.felix@unesp.br

1   School of Science and Engineering, Department of Civil Engineering, São Paulo State University (UNESP), Guaratinguetá, Brazil

2   Federal University of Latin American Integration (UNILA), Latin American Institute of Technology, Infrastructure and Territory, Foz do Iguaçu, Brazil

of the bond strength between steel and concrete, and spalling of the concrete cover.

According to Helene [4], carbonation-induced corrosion, known as uniform corrosion, is frequently seen in structures in metropolitan areas and can also occur in coastal regions, depending on the concentration of chloride ions in the atmosphere. The corrosive process caused by carbonation is divided into two phases: initiation and propagation. The changeover is marked by the depassivation of steel, as seen in Fig. 1.

Corrosion initiation finalizes when the reinforcement undergoes depassivation. Carbonation-induced corrosion occurs when carbon dioxide meets the steel surface. The carbonation process can be simplified as the chemical interaction between CO_2 and calcium hydroxide $(Ca(OH)_2)$ in the cement paste, resulting in the formation of calcium carbonate $(CaCO_3)$ [6, 20–22]. In addition, carbonation can decrease the porosity and permeability of concrete, leading to steel depassivation [17, 23, 24].

Following the loss of the steel protective layer, the propagation phase starts, which is marked by the pace of corrosion and the effectiveness of the concrete covering. These factors mainly influence the internal tensions that develop at the steel/concrete interface due to the formation of corrosion products [25, 26]. The concrete cover cracks due to the stress field created at the interface between the two materials due to the expansion produced by rust (corrosion products). Macro-cracks emerge due to tensile stress caused by rust development, leading to material degradation and decreased service life [25]. Du et al. [27] found that the mutual action of corrosion and external loading causes a decrease in the residual strength of the reinforcement, which is not directly proportional to the rate of steel cross-sectional loss.
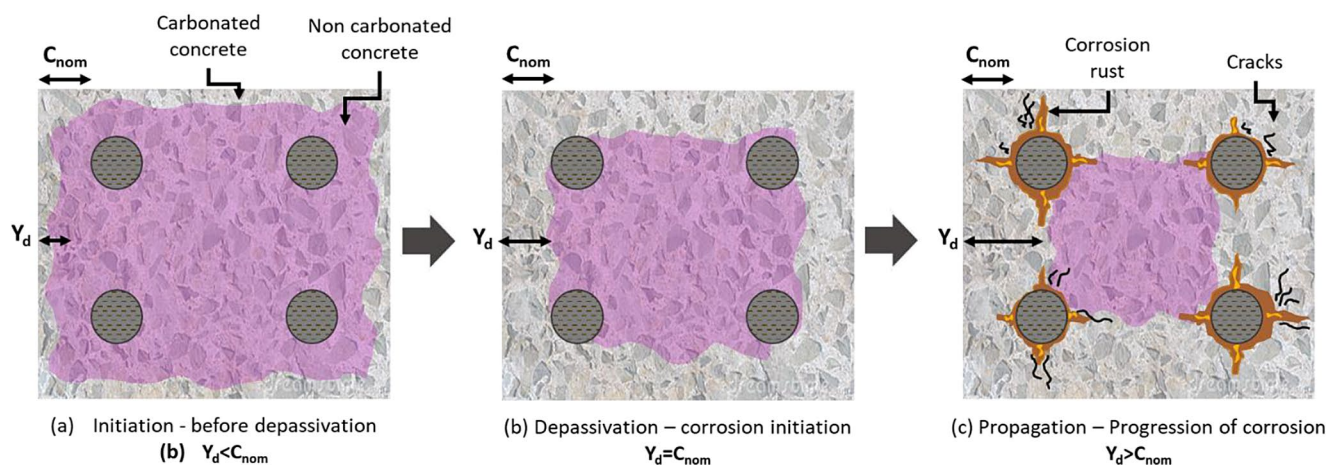
Regarding the modeling of carbonation-induced corrosion, most existing literature focuses on studying the initiation period of corrosion, particularly in developing models representing CO_2 diffusion in concrete or the time required for steel depassivation immersed in concrete [6, 10, 13, 21, 28–34]. Developing models for the initiation phase is important due accurately predicting the steel depassivation time allows for a more accurate assessment of the level of deterioration in reinforced concrete structures and the remaining service life of the composite material. Furthermore, employing these models in the design phase enables estimating the design working lives of a concrete structure and implementing measures to reduce reinforcement corrosion. This can be achieved by adjusting the concrete composition by including admixtures or inhibitor additives [35].

Despite several corrosion mapping models, estimations of steel depassivation periods still need to be improved associated with the models' lack of generality regarding exposure conditions and climatic aspects of the environment surrounding RC structures. Liberati et al. [36] and Ramezanianpour et al. [37] report the lack of representation of uncertainties associated with environmental climatic conditions, thus requiring the addition of random variables describing the variability of these parameters.

Ramezanianpour et al. [37] suggest using reliability theory analyses to improve the accuracy of estimating the probability of corrosion or steel depassivation to address the absence of parameter variability in deterministic models. This involves incorporating factors related to the randomness of variables affecting the issue. Ramezanianpour et al. [37] state that deterministic methods may produce unreliable findings when the environmental conditions around the RC structure substantially change.

Multiple techniques are available to assess the performance and durability of RC structures when faced with changes in their mechanical and physical characteristics [38–41]. The Monte Carlo simulation technique is a solid way to analyze problems by considering multiple random factors [42, 43]. Integrating mathematical diffusion laws

Fig. 1 Stages of corrosion induced by carbonation. Adopted from Felix and Carrazedo [19]

with reliability algorithms provides a practical approach for modeling the service life of concrete structures affected by corrosion, yielding more dependable and thorough results than deterministic estimates [14, 36–38, 43, 44].

Therefore, considering the increasing use of reliability theory in the probabilistic analysis of structural component failure due to various deterioration mechanisms, especially reinforcement corrosion, this work presents a framework for analyzing the design life of RC structures subjected to carbonation-induced corrosion. As an original contribution, we propose an approach that combines a carbonation depth model based on Artificial Neural Networks with the Monte Carlo simulation technique, utilizing only data from concrete elements exposed to natural degradation conditions. The carbonation depth model was created using feedforward Multilayer Perceptron ANNs (MLP-ANN) with the backpropagation algorithm. The model was trained on a database of 870 data points derived from natural carbonation results found in the literature. These sources encompassed studies that measured carbonation depths in concrete under various natural environmental conditions and are related to concrete elements located in nine countries with different weather conditions. The depassivation probability was calculated using reliability theory principles and the ANN-based model of carbonation depth, where a case study is offered to showcase the technique's efficiency.

2 Probabilistic approach

Figure 2 illustrates the two main methodological processes adopted in the approach development: (i) building an ANN-based model for mapping the concrete carbonation front and (ii) coupling the Monte Carlo Simulation technique with the carbonation model. The following subsections detail all the processes used to define the probabilistic approach.

2.1 Building the carbonation model based on ANN

2.1.1 Data analysis and processing

It is crucial to ensure the reliability of the database used within an artificial neural network model to train it effectively. The database was meticulously built based on 870 literature sources [6, 13, 45–53]. These sources included studies that measured carbonation depths in concrete under various natural environmental conditions and encompassed concrete elements from nine countries with diverse weather conditions (Brazil, Canada, China, Estonia, USA, France, India, Portugal, and Taiwan).

As known, several parameters influence the process of concrete carbonation, including the composition of the binder, concrete mix design, environmental conditions, and exposure time. In this study, ten parameters have been identified and selected as input parameters for the model: the average proportion of clinker + gypsum in the cement "CG+" (in %), concrete's compressive strength at 28 days "CS" (in MPa), type of admixture "TADMIX" (0 - concrete without admixture; 1 – with blast furnace slag; 2 – with fly ash; 3 – with limestone filler; 4 – other pozzolanic materials; 5 – silica fume), the admixture-cement ratio "AMDIX" (in %), CO_2 concentration in the atmosphere "CO2" (in %), annual average relative humidity "RH" (in %), annual average temperature "TEMP" (in °C), exposure condition "EXP" (0.65 – outdoor, exposed to rain; 1.0 – outdoor, sheltered from rain; 1.3 – indoor), the water-binder ratio "W/B", and exposure time "TIME" (in years). Figures 3 and 4 illustrate the dispersion of the feature values with the
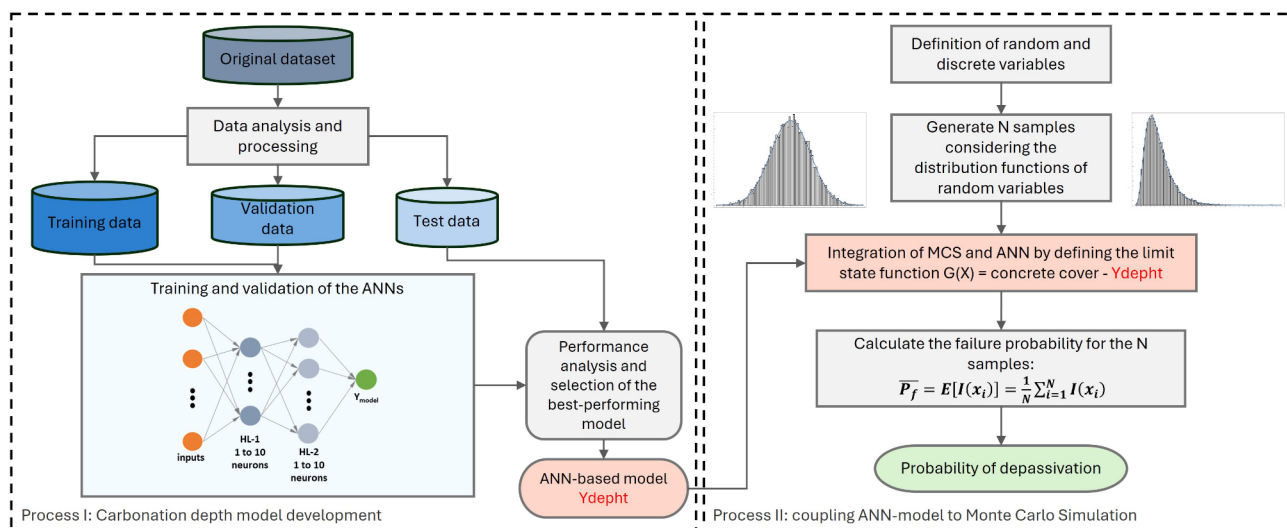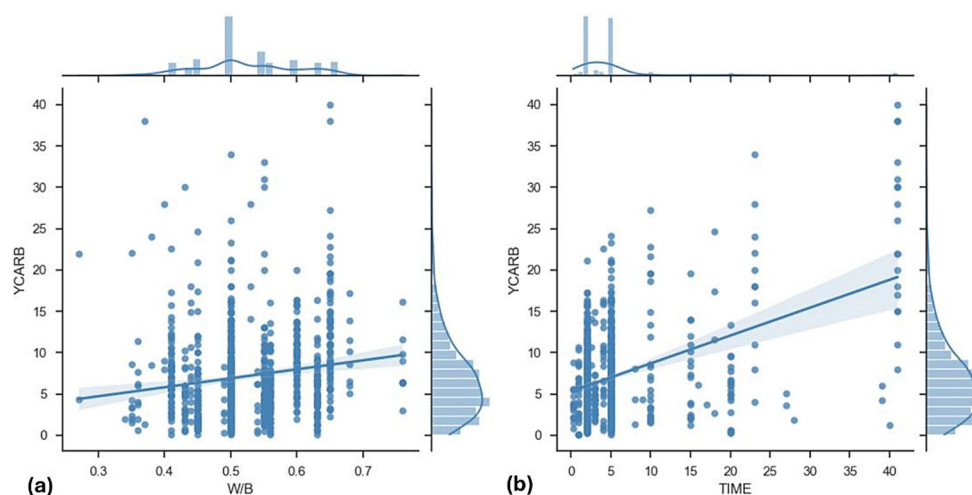

Fig. 2 Flowchart of the main methodological processes

Fig. 3 Dispersion and distribution graphs of (**a**) water-binder and (**b**) exposure time

carbonation depth and frequency distribution of all continuous variables of the original database. Table 1 provides the maximum, minimum, average, and standard deviation values. Since EXP and TADMIX are discrete variables, their histograms were not plotted, and statistical parameters were not defined.

As shown in Fig. 3a, 51% of the database had a water-binder ratio varying from 0.45 to 0.65. Figure 4c shows that the proportion of admixtures varies between 0 and 60% and that three peaks exist, indicating more than one high frequency in the data. The histograms of CS (ranging from 14.3 to 84.3 MPa), TIME (ranging from 0.25 to 41.0 years), and YCARB (ranging from 0.07 to 40.0 mm) exhibit right skewness. For relative humidity and temperature, in Fig. 4e, f, there is more than one peak in the concentration of data, and the most significant proportion of data is located close to the average values.

Figure 5 displays a Pearson correlation matrix among all variables, offering further insight into the database. The matrix shows no stronger correlations between the input features and the carbonation depth (YCARB). The data analysis points out that the carbonation depth exhibits moderate relationships with the exposure time (0.52), water-binder ratio (0.40), concrete's compressive strength (-0.37), and annual average temperature (0.27), indicating that these parameters directly influence the carbonation depth mapping. It is important to note that temperature showed a median positive linear correlation with carbonation depth, suggesting the importance of considering it when mapping natural carbonation.

After defining the dataset and the input features model, the data was scaled to a range of 0 to 1 to enhance the performance and accuracy of the networks. The dataset was split into two subsets for modeling: one including 80% of the data for training and cross-validation using a 10-fold approach for the ANN, and another containing 20% for

testing the model and assessing its actual performance. This method is crucial as it evaluates the model's generalization capacity more accurately by minimizing the chances of overfitting to a particular data subset [54–56]. The data split was done using stratified sampling to preserve the database patterns [57].

2.1.2 Training, validation, and performance test

Artificial Neural Networks emulate the human brain, comprising interconnected layers of artificial neurons [58]. Neurons process weighted inputs, apply non-linear activation functions, and transmit outputs to subsequent layers (Fig. 6a). The ANN architecture features input, hidden, and output layers, with weights adjusted during training using optimization algorithms like gradient descent. ANNs excel at learning complex data patterns and performing tasks such as classification, regression, and natural language processing, with applications spanning image recognition, speech processing, medical diagnosis, and financial forecasting, showcasing the versatility of machine learning.

The MLP, a specific ANN type, consists of multiple interconnected layers of neurons, including input, hidden, and output layers (Fig. 6b). Backpropagation is a pivotal technique for training MLPs, enabling them to learn from data and make predictions. Modeling an MLP with backpropagation entails defining the network architecture, initializing parameters, and training the network by feeding input data forward and comparing the output to target values using a chosen loss function. Backpropagation updates network parameters by computing error gradients and adjusting parameters using optimization algorithms. This iterative process is repeated for multiple epochs until convergence, resulting in an accurate MLP model capable of capturing complex data patterns and making precise predictions. The

Fig. 4 Data dispersion and distribution considering: (**a**) proportion pf clinker + gypsum in the cement; (**b**) concrete's compressive strength; (**c**) admixture-cement ratio; (**d**) CO_2 concentration; (**e**) relative humidity and; (**f**) temperature
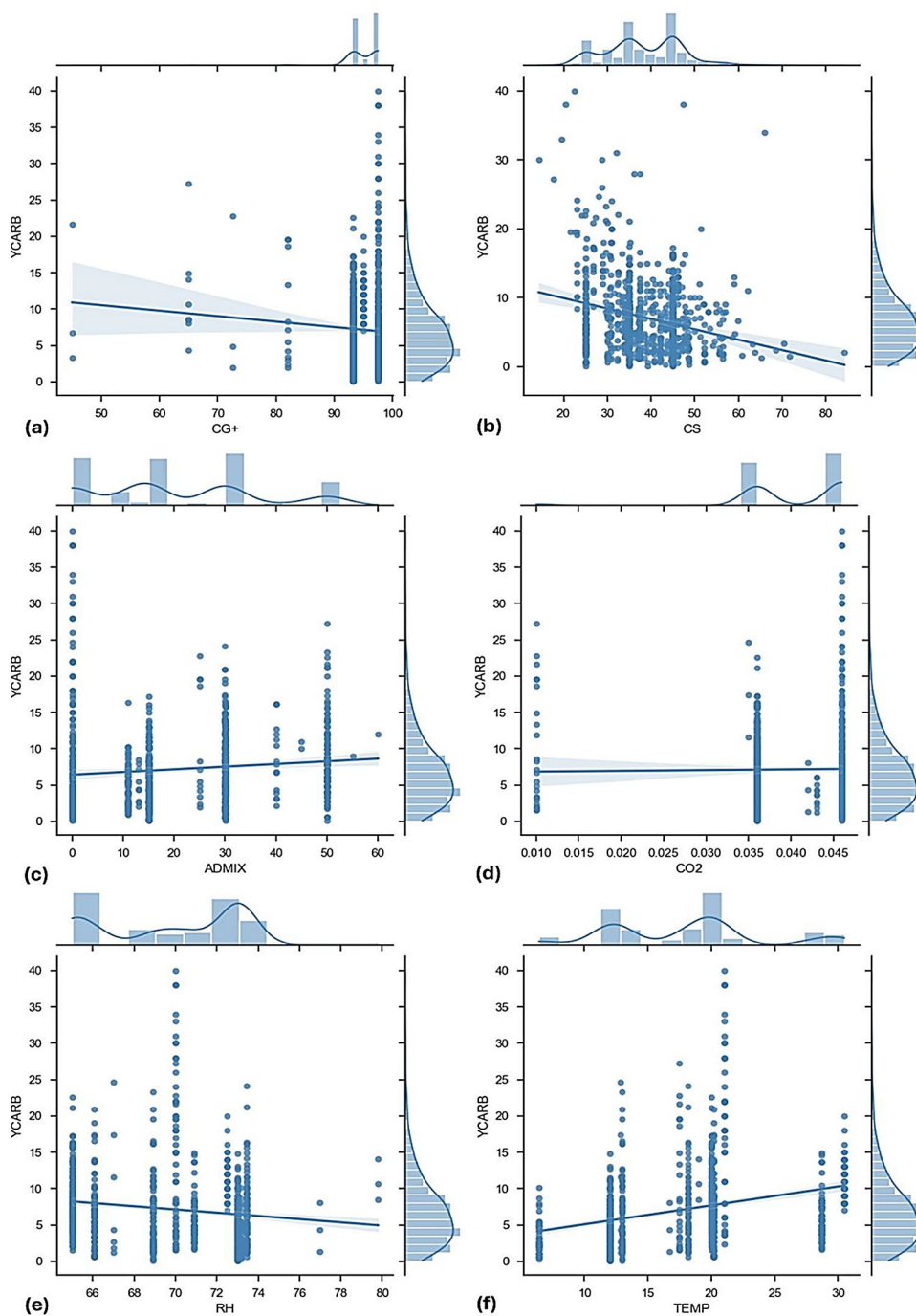
Table 1 Statistical parameters of the continuous features

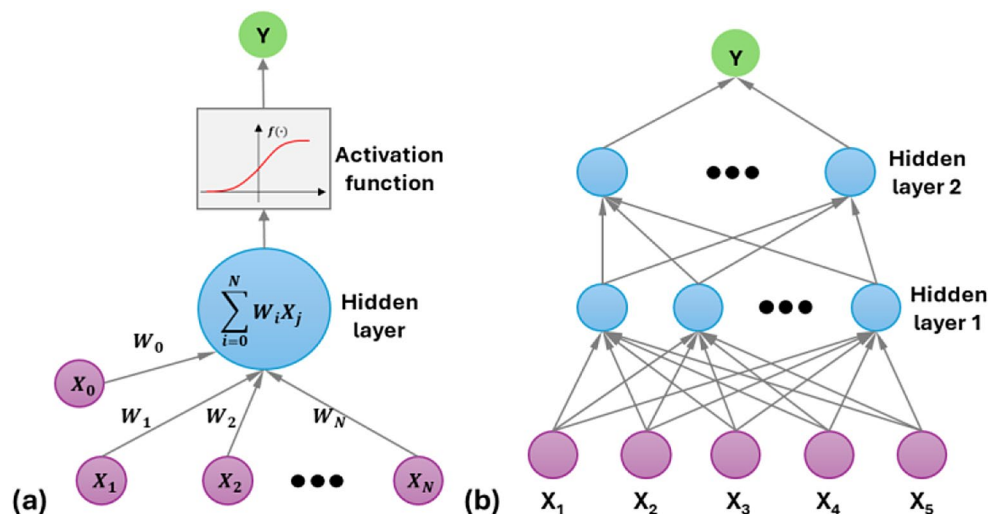| Feature	Unit	Minimum	Maximum	Average	Standard deviation
proportion of clinker + gypsum (*CG+*)	%	45.00	97.50	94.73	5.01
compressive strength at 28 days (*CS*)	MPa	14.30	84.30	38.44	8.83
admixture-cement ratio (*ADMIX*)	%	0.00	60.00	20.02	16.11
CO_2 concentration (*CO2*)	%	0.01	0.046	0.040	0.007
annual average relative humidity (*RH*)	%	65.00	79.80	69.83	3.41
annual average temperature (*TEMP*)	°C	6.40	30.50	17.98	6.13
water-binder ratio (*W/B*)	-	0.27	0.76	0.52	0.07
exposure time (*TIME*)	years	0.25	41.00	5.50	7.08
Carbonation depth (Y_{CARB})	mm	0.07	40.00	7.16	5.44
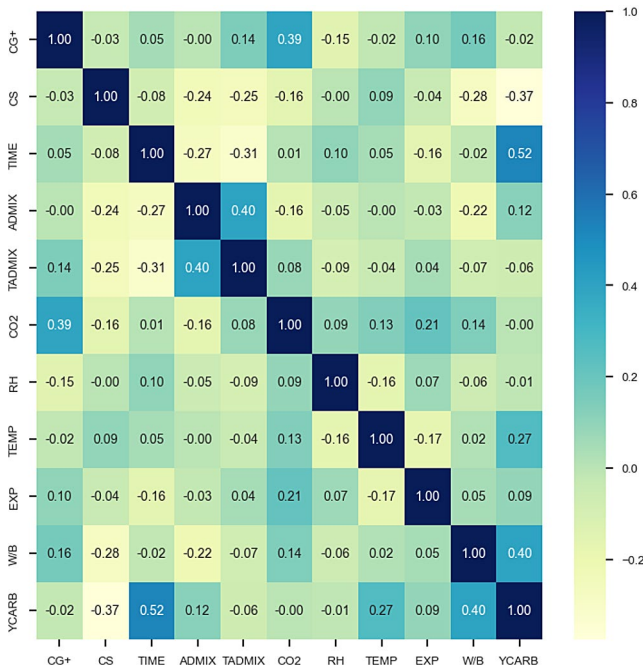
Fig. 5 Pearson correlation matrix

trained model enables various classification, regression, and pattern recognition applications.

Several topologies were tested in this work, differing by the number of neurons in the two hidden layers. The number of neurons varied from 1 to 10 in the first and second hidden layers. The topologies were defined to have low complexity, ensuring that all ANNs have a maximum of 20 neurons. To analyze the influence of topology, the initial weights were defined at 0.5 in all training processes.

Considering that supervised learning with the backpropagation training algorithm was utilized, it was necessary to establish a learning rate since it is directly associated with the network's convergence rate [59]. Based on Felix et al. [13], the learning rate and momentum variable were fixed

at 0.4 and 0.7, respectively. The hyperbolic tangent function was defined as the activation function in all training, and the mean square error was established as a training convergence criterion, with a maximum of 10^6 iterations.

After training all the ANNs, a performance analysis was conducted to define the model with the best prediction and generalization, in which the coefficient of determination (R^2) and the root-mean-square error (RMSE) were evaluated, using Eqs. 1 and 2, respectively.

$$R^2 = \left(\frac{\sum_{i=1}^{n} \left(O_i - \overline{O} \right) \left(Y_i - \overline{Y} \right)}{\sqrt{\sum_{i=1}^{n} \left(O_i - \overline{O} \right)^2} \sqrt{\sum_{i=1}^{n} \left(Y_i - \overline{Y} \right)^2}} \right)^2 \tag{1}$$

$$RMSE = \sqrt{\frac{1}{n} \sum_{i=1}^{n} \left(O_i - Y_i \right)^2} \tag{2}$$

in which Y_i are the real values and O_i are the model predictions. n is the amount of data samples evaluated, $\overline{Y}$ are the average of real values and $\overline{O}$ represent the means of model outputs.

2.2 Probabilistic modeling

Monte Carlo simulation is a computational method for conducting reliability analysis [36, 45, 60]. This method utilizes random samples to characterize the probability of failure (that in this work means the depassivation probability), as shown in Eq. (3).

$$P_f = \int_{G \leq 0} f_x \left(x_1, x_2, \ldots, x_n \right) dx_1, dx_2, \ldots, dx_n \tag{3}$$

Fig. 6 (**a**) Perceptron ANN and (**b**) MLP-ANN with two hidden layers

where Pf is the failure probability, $f_x(X)$ is the joint probability density function (joint PDF) of the variables X.

The failure probability is calculated using samples created according to the statistical distribution associated with the problem's random variable. This strategy, founded on simulating the limit state function, uses a larger sample size to depict the probability of failure or establish reliability accurately [61].

Calculating the integral in Eq. (3) is challenging and requires using different methods and procedures that rely on the dependability index β [61]. The reliability index is defined as the distance between the midpoint and the point of failure allocated on the limit state function, G(X) = 0, and it is related to the probability of failure through the cumulative standard normal distribution function ϕ, as Eq. (4).

$$P_f = \phi\left(-\beta\right) \tag{4}$$

The Monte Carlo simulation method involves generating samples for the random variables related to the issue. The probability of failure is determined by an estimator that evaluates the limit state function, following Eq. (5). Estimator I(xi) is calculated using Eq. (6), assuming 1 or 0, representing failure or not, respectively.

$$
\begin{aligned}
P_f &= \int_{G \le o} f_x\left(x_i\right) dx_i \\
&= \int_{G \le 0} I\left(x_i\right) f_x\left(x_i\right) dx_i \\
&= E\left[I\left(x_i\right)\right]
\end{aligned}
\tag{5}
$$

$$
I\left(x_i\right) = \begin{cases} 1, & G\left(X\right) \le 0 \\ 0, & G\left(X\right) > 0 \end{cases}
\tag{6}
$$

The average value $I(x_i)$ will be an estimative for the probability of failure, so, according to Eq. (7), the failure probability can be estimated for the entire sample database.

$$\overline{P_f} = E\left[I\left(x_i\right)\right] = \frac{1}{N}\sum_{i=1}^{N} I\left(x_i\right) \tag{7}$$

where N is the number of simulations and evaluations of the limit state equation. In this work, samples were defined by the Importance of Sample technique. According to Jacquemart et al. [62]. The Importance Sample is an interesting theoretical approach to estimating rare event probabilities in a continuous Markov process.

Once the method for determining the probability of failure (that means depassivation) is established, the only task remaining is to define the limit state equation $G(X)$. The ANN-based model of carbonation depth, with the best performance, was integrated with the Monte Carlo simulation algorithm defining $G(X)$, as presented in Eq. (8).

$$G\left(X\right) = C_{non} - f_{ANN}\left(X_R, X_D\right) \tag{8}$$

where X is the vector of random and discrete variables, C_{non} is a random variable associated with the concrete cover thickness (mm), f_{ANN} is the ANN-based model of carbonation depth, X_D is the vector of discrete variables (gypsum in the cement in %, type of admixture, the admixture-cement ratio in %, exposure condition, the water-binder ratio, and exposure time in years) and, X_R is the vector of discrete variables (concrete's compressive strength at 28 days in MPa, CO_2 concentration in the atmosphere in %, annual average relative humidity in %, annual average temperature in °C).

3 Results and discussion

3.1 Carbonation model based on ANN

The probabilistic approach proposed in this work uses a model with Artificial Neural Networks to calculate the concrete carbonation depth. Thus, an ANN-based model was established using the training strategy explained in the preceding section. After training all 100 ANNs, a performance study was undertaken to identify the architecture that provides the best learning and generalization. The coefficient of determination (R^2) was assessed during the training and test phases and displayed in contour maps, as seen in Figs. 7 and 8.

The results in Figs. 7 and 8 demonstrate that the generalization capacity (values of R^2 obtained in the test phase) was lower than the learning ability (R^2 obtained in the training phase) for mapping carbonation depth. While in the training phase, the ANN model with the topology [10-10-9-1][1] generated the best learning, with a training R^2 of 0.952, in the test phase, the ANN [10-6-8-1] generated the best generalization with an R^2 of 0.849. With the best learning, the ANN [10-10-8-1] generates an ANN with R^2 of 0.252 in the test phase. These findings indicated a potential mismatch between generalization and learning capacity, complicating the determination of which ANN produces the best results when assessing the R^2 of the test or training separately. It was therefore decided to use a new performance metric that considers both training and test performance, as well as the error metrics RMSE, obtained in both phases, as the goal

---

[1] The ANN topology in this study is represented by the notation [X-Y-Z-W], where X is the number of model inputs (fixed at 10), Y is the number of neurons in the first hidden layer, Z is the number of neurons in the second hidden layer, and W is the number of model outputs (always one).
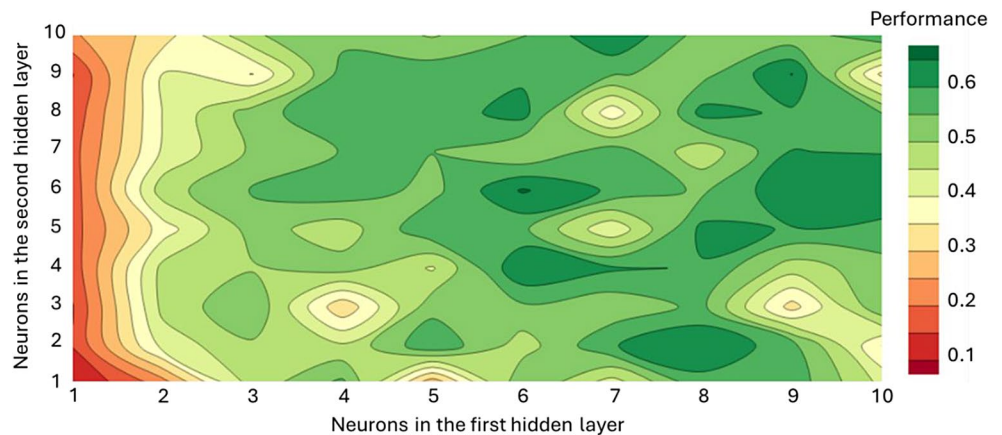
Fig. 7 R² values obtained in the training phase as a function of the ANN topology
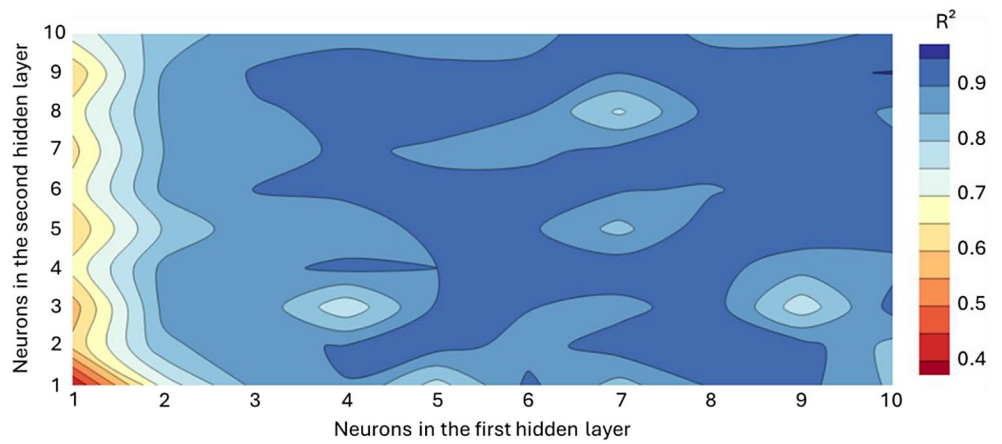
Fig. 8 R² values obtained in the test phase as a function of the ANN topology
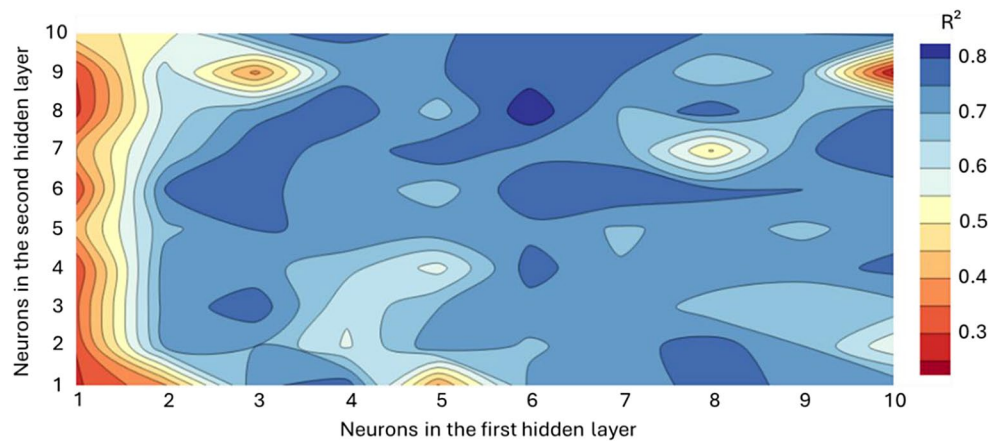
**Fig. 9** Weighted performance values as a function of the ANN topology

of this work is to propose an approach with overall applicability for durability analysis in RC structures subjected to corrosion induced by carbonation. The equation defined and used in this study, presented in Eq. 9, combines the R² and RMSE values of the training and test phases to evaluate the network with the best performance. It gives more weight to the metrics values obtained during the test phase, resulting in a model with a reasonable degree of generalization. Figure 9 shows the performance values calculated by Eq. 9.

$$Weighted\ Performance = \frac{0.6R^2_{TES} + 0.4R^2_{TRA}}{0.6RMSE_{TES} + 0.4RMSE_{TRA}} \quad (9)$$

in which R^2_{TRA} and R^2_{TES} are the R² values obtained in the training and test phases, respectively. $RMSE_{TRA}$ and $RMSE_{TES}$ refer to the RMSE values obtained in the training and test phases, in that order.
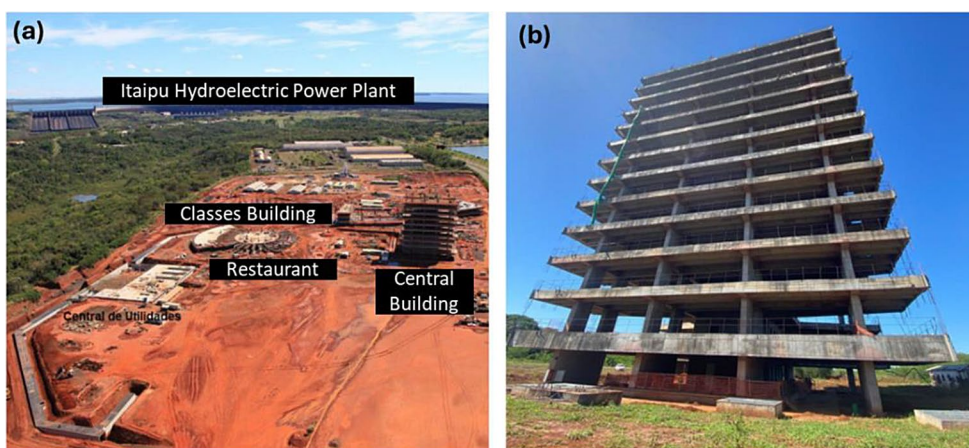
Figure 9 shows that the ANN with the highest performance is configured by [10-6-6-1] topology, whose metric calculated by Eq. 9 is 0.67. The ANN [10-6-6-1] obtained
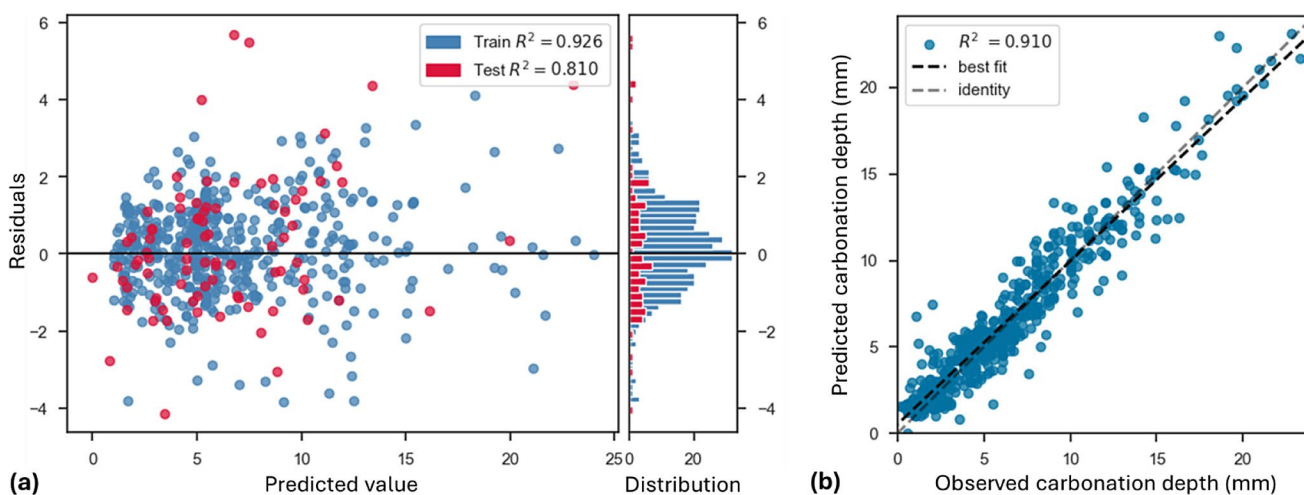
Fig. 10 (**a**) residuals plot and (**b**) observed-prediction correlation plot

Fig. 11 (**a**) General view of the building site and (**b**) structure of the Central Building [63]

an R² of 0.926 in the training and 0.810 in the test, with an overall performance of 0.910, as presented in Fig. 10. The model's RMSE is 1.288 mm, with a maximum error of 5.686 mm.

3.2 Probabilistic analysis – case study

The developed approach's performance is assessed through a case study analyzing the design life of RC structures in the Central Building of the Campus of the Federal University of Latin American Integration, situated within the security perimeter of the Itaipu Hydroelectric Power Plant in Foz do Iguaçu - Paraná, Brazil. The construction commenced in 2011 and was suspended in 2014. The data utilized in the case study were sourced from architectural and structural projects, descriptive memoranda, and technological control reports available in [63, 64] (See Fig. 11).

The Central Building's RC structures were built using a combination of reinforced and prestressed concrete, with compressive strengths ranging from 35 MPa to 50 MPa. All concrete utilized was produced at an on-site concrete batching plant, utilizing Brazilian Cement Portland CP IV, comparable to CEM IV (Portland cement with pozzolan). Three structural elements from the Central Building were chosen for the design life analysis: a wall-pier, a Column, and a beam. The data of these elements is presented in Table 2. Additional information regarding the structures is available in Possamai [63] and Possan et al. [64].

Possamai [63] analyzed the concrete technological-control reports from 2012 to 2014 to evaluate the variability of concrete's compressive strength (CS) by treating it as a random variable. The data included six specimens tested at 7 days and 28 days. The analysis focused on concrete strength values at 28 days, with two specimens from distinct batches examined for each typical design strength of 35 and 50 MPa. This process yielded 330 batches for $CS \geq 35$ MPa and 410 for $CS \geq 50$ MPa. Distribution curves and histograms, treated as normal probability distribution functions, are depicted in Fig. 12.

Table 2 Information on the assessed RC components [63]

Structural element	Location of RC structure in Central Building's	Concrete cover thickness (mm)	Compressive strength (MPa)	W/B	Exposure conditions
Wall-Pier	Ground floor	2.0	50.00	0.55	outdoor, exposed to rain
Column	11th floor	2.5	35.00	0.50	outdoor, sheltered from rain
Beam	2nd floor	2.5	35.00	0.50	outdoor, exposed to rain
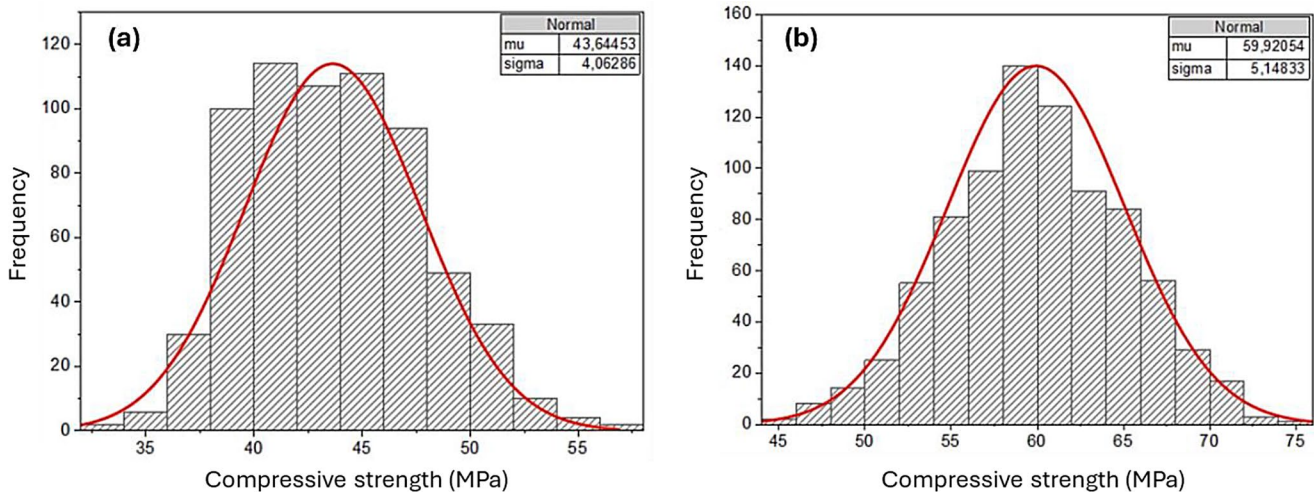
Fig. 12 CS distribution curve for concretes with (**a**) 35 MPa and (**b**) 50 MPa [63]

Table 3 Specifications of random variables. Fonte Possamai (2022)

Structural element	Variable	Mean	Standard deviation
Wall-Pier	CS (MPa)	59.920	5.1480
	C_{non} (mm)	20.000	2.0000
	CO_2 (%)	0.0410	0.0043
	RH (%)	74.317	8.5084
	$TEMP$ (°C)	24.334	6.9532
Column	CS (MPa)	43.640	4.0630
	C_{non} (mm)	25.00	2.5000
	CO_2 (%)	0.0410	0.0043
	RH (%)	74.317	8.5084
	$TEMP$ (°C)	24.334	6.9532
Beam	CS (MPa)	43.640	4.0630
	C_{non} (mm)	25.000	2.5000
	CO_2 (%)	0.0410	0.0043
	RH (%)	74.317	8.5084
	$TEMP$ (°C)	24.334	6.9532

The average value of the cover thickness (Cnon) was determined based on the project parameters, accounting for a 10% variation with a normal distribution function. Based on these numbers, we implemented appropriate quality control measures during the execution phase in alignment with Enright and Frangopol [65].

Climatic data on annual average relative humidity (*RH*) and annual average temperature (*TEMP*) were gathered from 2010 to 2023, spanning a 13-year period. The data was pulled from the meteorological database for Teaching and Research (BDMEP) of the National Institute of Meteorology (INMET) [66]. Daily data from station A846, located in Foz do Iguaçu, were obtained, and annual averages were calculated. Finally, for the characterization of CO_2 exposure, data on Brazilian CO_2 concentration were considered, according to the "CO_2 levels" organization [67], due to the absence of data for the city of Foz do Iguaçu, PR. Table 3 presents the means and standard deviations for the aforementioned parameters. The normal distribution function was utilized to define all the random variables.

The first step in the probabilistic analysis involves determining the number of samples and simulations necessary to ensure dependable outcomes. As Liberati et al. [36] outlined, the failure probability of civil structures typically falls within the range of 10^{-3} to 10^{-6}, necessitating approximately 10^5 to 10^9 limit state simulations. Alternatively, a convergence study is another effective method to reduce computing workload. Thus, a study assessed the impact of sample size on assessing the depassivation probability of the Wall-Pier (Table 3) considering a 100-year analysis period. Figure 13 shows the convergence analysis results for the variability of the probability of depassivation over 100 years, with the number of samples used in the simulations.

The results shown in Fig. 13 suggest that the probability of failure tends to stabilize at 0.0086 for samples greater

Fig. 13 Number of samples versus depassivation probability of the Pilar structure
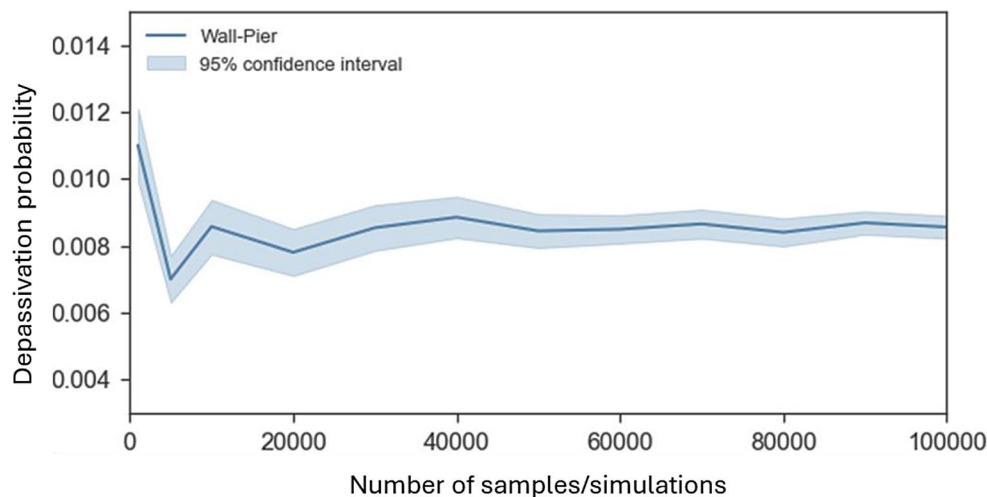
Fig. 14 Depassivation probability or RC structures
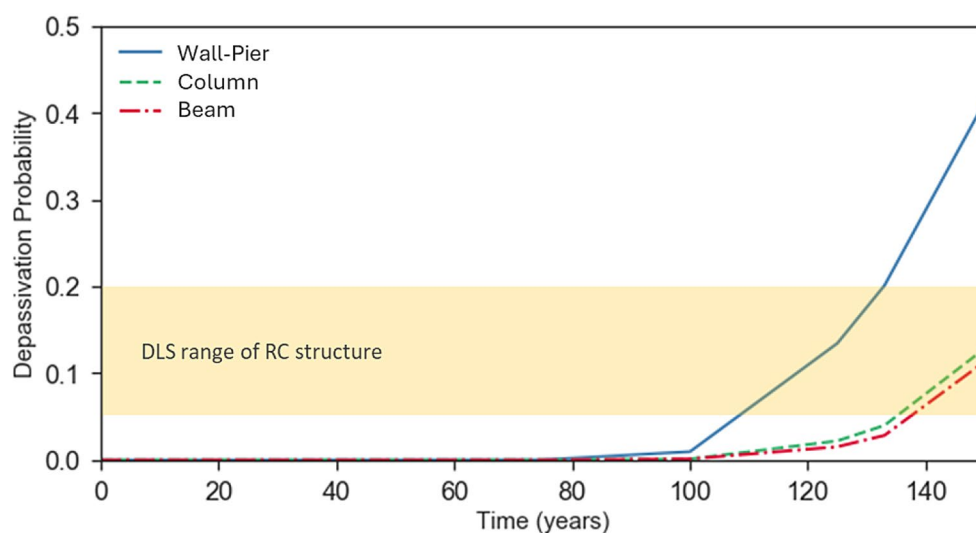
than 40,000. Thus, this study utilized 50,000 samples to perform a Monte Carlo simulation for each RC structure.

Once the number of samples required had been determined, simulations were carried out to estimate the probability of the structures collapsing. Figure 14 shows the probabilities of steel depassivation due to concrete carbonation. The analyses were carried out for 150 years, with a value three times longer than the design service life (50 years for RC structures) defined in the Brazilian performance standard NBR 15575-1 [68]. In addition, Figs. 15, 16 and 17 show the distributions of the carbonation depth values predicted by ANN and the concrete cover, considering the variables' randomness and the region where the limit state equation is exceeded.

According to the results shown in Fig. 14, within a period of 150 years, the probability of depassivation (PD) of the structures does not reach 50%. The results show that durability in the face of carbonation is greater in the Column (PD = 0.128) and the Beam (PD = 0.113), with the probability of depassivation in these structures being less than 20%

of the probability in the Wall-Pier (0.412). The probability of depassivation is close to zero for the first 50 years of life, indicating that the structures' durability limit state (DLS) is not reached during the design life. This observation is independent of the concrete used in the structural element and the conditions of use of the RC structure.

According to the general principles on the design of RC structures for durability on ISO 13,823 [69]. The durability limit state is reached when the probability of depassivation is 0.05 to 0.2 (indicated in a yellow band in Fig. 14). Thus, the design service life of the evaluated structures is 109 years for the Wall-Pier (PD = 0.051), 136 years for the Column (PD = 0.0504), and 139 years for the Beam (PD = 0.051).

The Wall-Pier's lower durability may be partly linked to the established definition of environmental aggressiveness in the structure's design, which specified a concrete cover thickness of 20 mm. With a 25 mm concrete cover, the structure would have a depassivation probability of 0.137 at 150 years, exceeding the design service life of 132 years by 21% compared to employing a 20 mm cover. It is crucial to
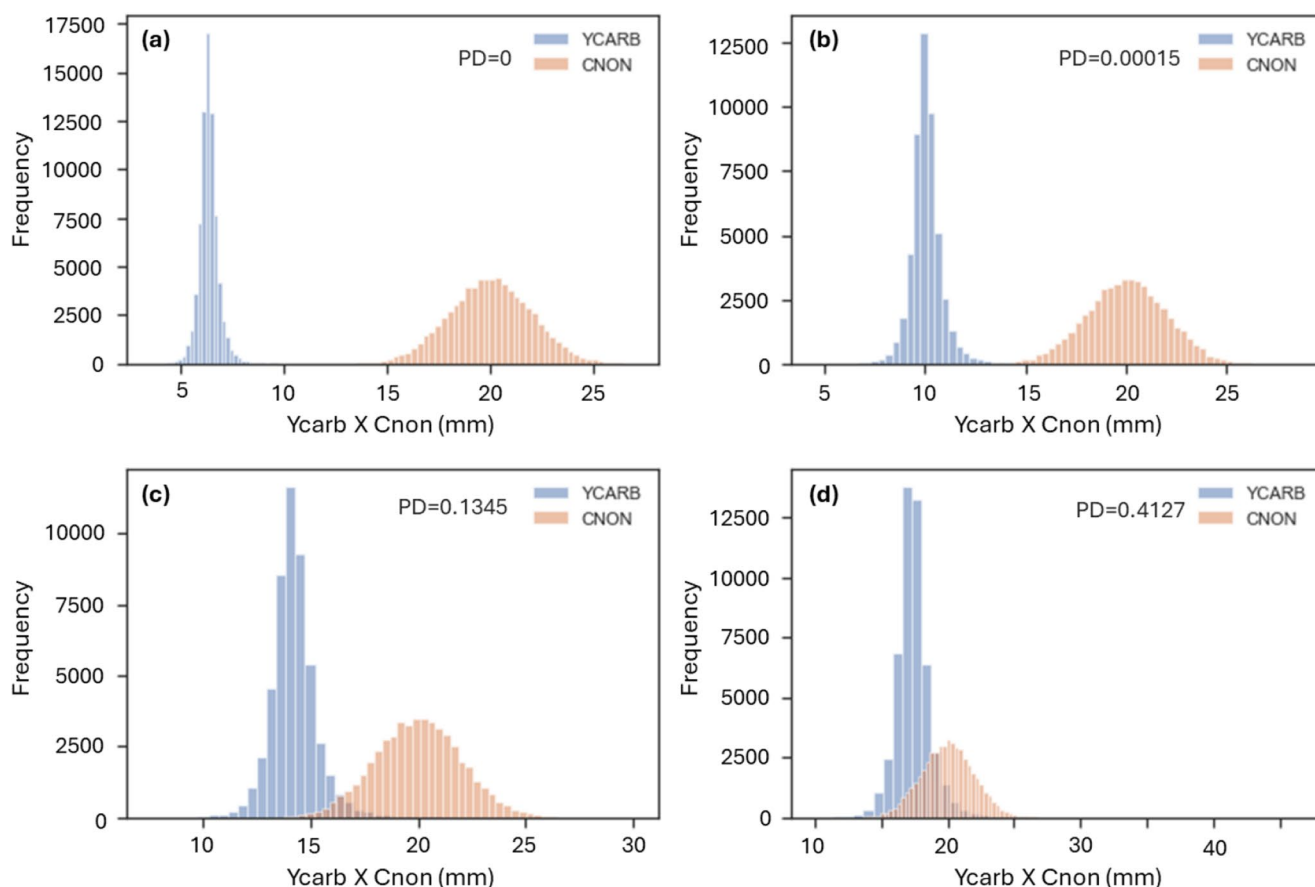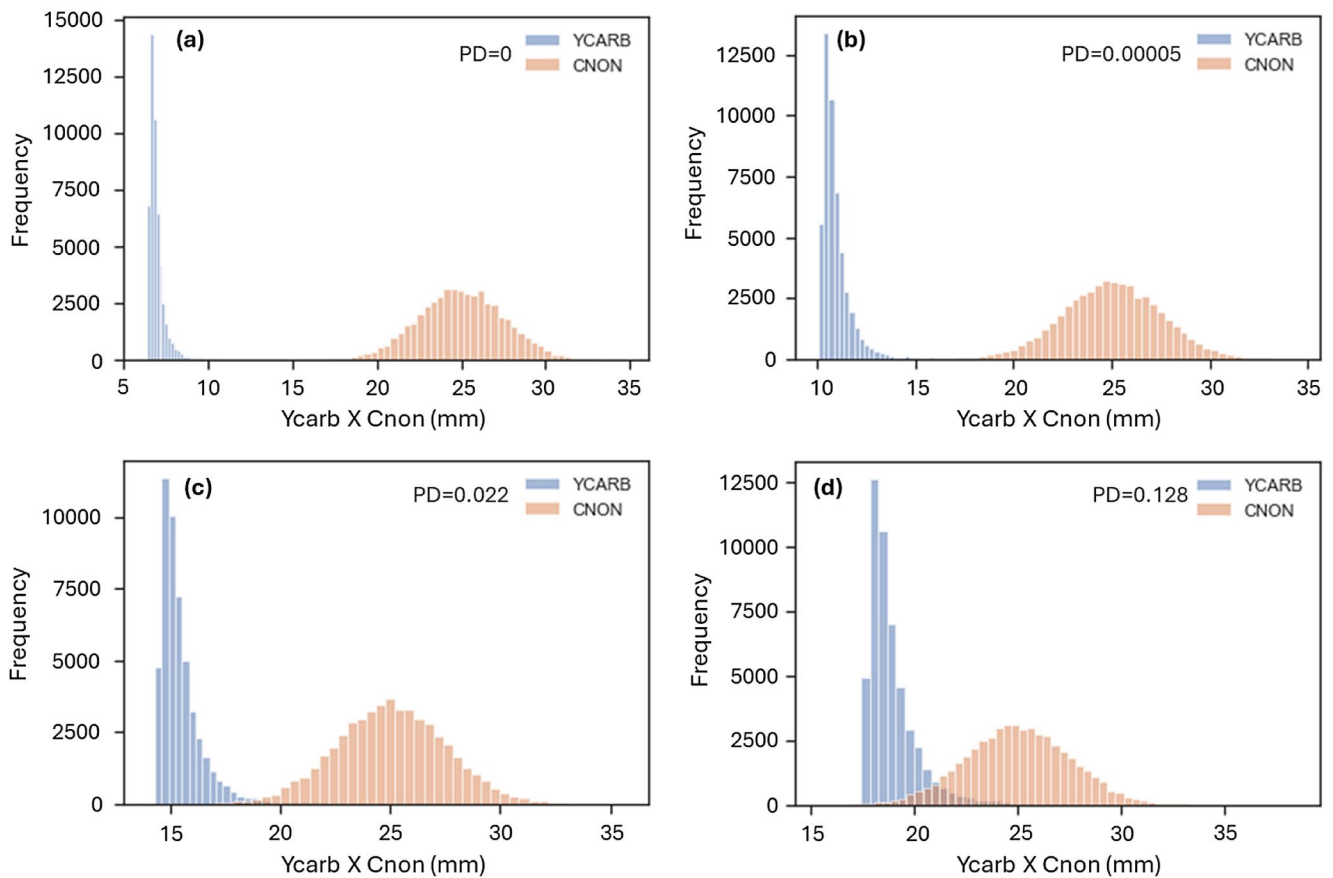
Fig. 15 Carbonation depth and cover thickness distributions for the Wall-Pier structure at (**a**) 50 years, (**b**) 75 years, (**c**) 125 years, and (**d**) 150 years

accurately assess the hostile environment during the design phase to select a suitable cover thickness.

According to the results shown in Figs. 13, 14, 15, 16 and 17, the design service life (50 years) recommended in NBR 15575-1 [68] is guaranteed for the three structures evaluated, and according to the DLS indicated in ISO 13,823 [69], the design service life is between 109 and 139 years. Nevertheless, these findings were derived from a probabilistic analysis, an approach not widely used in the country for projects and durability studies. Durability analyses are typically conducted using deterministic studies that do not account for parameter uncertainties. Figure 18 shows the predicted carbonation depth for the three reinforced concrete structures using the proposed artificial neural network model. The predictions were established using the average values of the input parameters according to Tables 2 and 3.

Figure 18 shows that depassivation is not expected during the 150-year period for any RC structures. The predicted

carbonation depths were 15.16 mm for Wall-Pier, 18.65 mm for the Column, and 20.15 mm for the Beam. The proposed model suggests that the design service life for the Wall-Pier would be 259 years, 272 years for the Column, and 236 years for the Beam, based on deterministic analysis. Figure 18 shows that the carbonation process occurs at a slower rate in the Wall-Pier; however, as this structure was produced with a smaller cover (20 mm) compared to the Beam and the Column structures (with 25 mm of concrete cover), the probabilistic analysis resulted in a shorter design life. The results in Figs. 14 and 18 highlight the necessity of including probabilistic analyses in examining durability and design service life. The deterministic analysis could lead to depassivation of the reinforcement occurring up to 238% later than indicated by probabilistic analyses. This discrepancy could result in inaccurate durability assessments, particularly in severe conditions or lower performance concretes.

Fig. 16 Carbonation depth and cover thickness distributions for the Column structure at (**a**) 50 years, (**b**) 75 years, (**c**) 125 years, and (**d**) 150 years

At last, a parameter analysis was carried out on the proposed model to investigate the influence of the concrete cover thickness on RC structures' durability and approach performances. Nominal covers of 15, 20, 25, and 30 mm were evaluated for the Wall-Pier RC structure. Figure 19 shows the results of this analysis.

According to Fig. 19, decreasing the concrete cover of the Wall-Pier Structure by 25% (from 20 to 15 mm) would lead to a 48% decrease in the structure's design life, reducing it from 109 years to 56 years. These results highlight the significance of accurately determining and implementing the thickness of the cover for the structure. This is crucial as any movements in the structure's formwork system during molding can displace spacers, resulting in covers that deviate from the intended design, as reported by According to Palm et al. [70], which indicated that a combination of concrete cover and construction best practices must be incorporated into every project to enhance the structure's durability and lifespan.
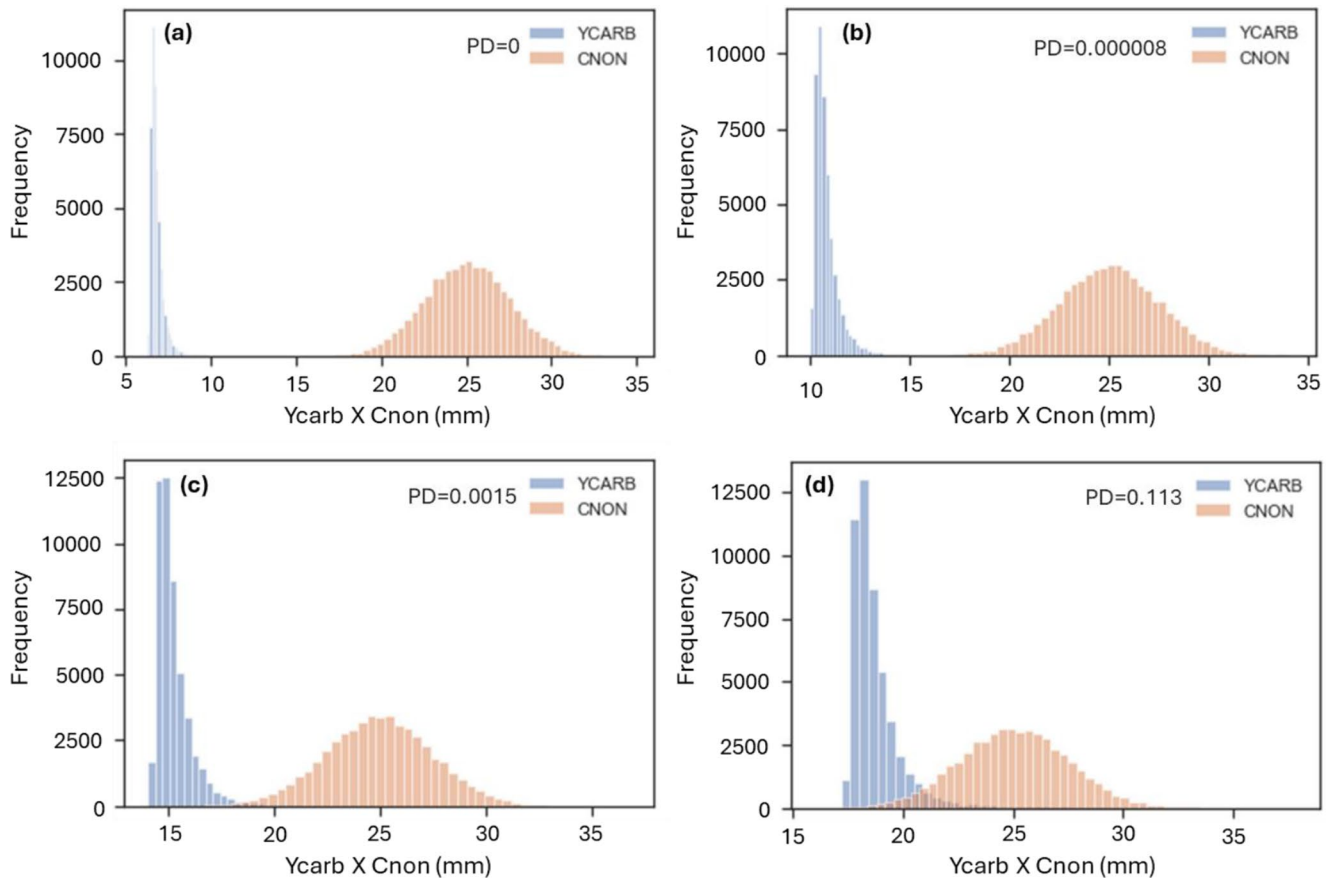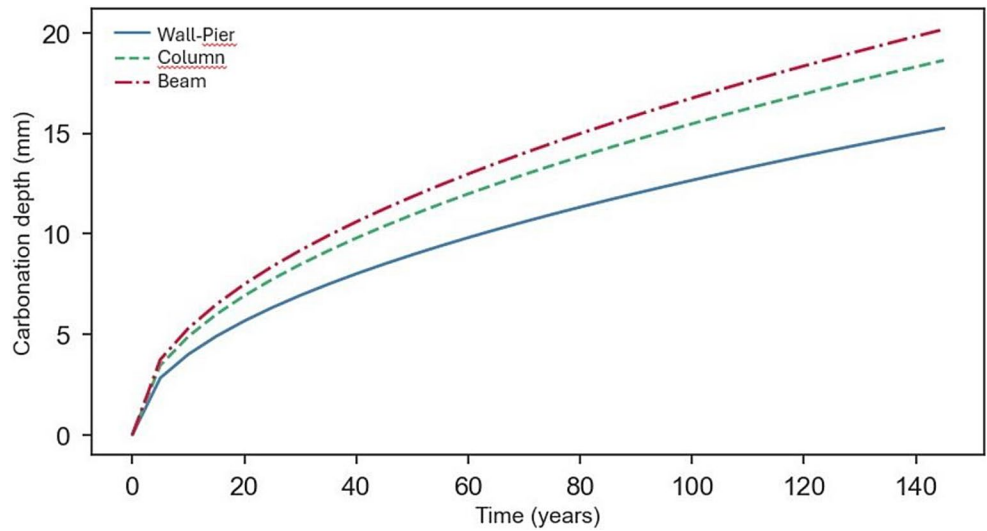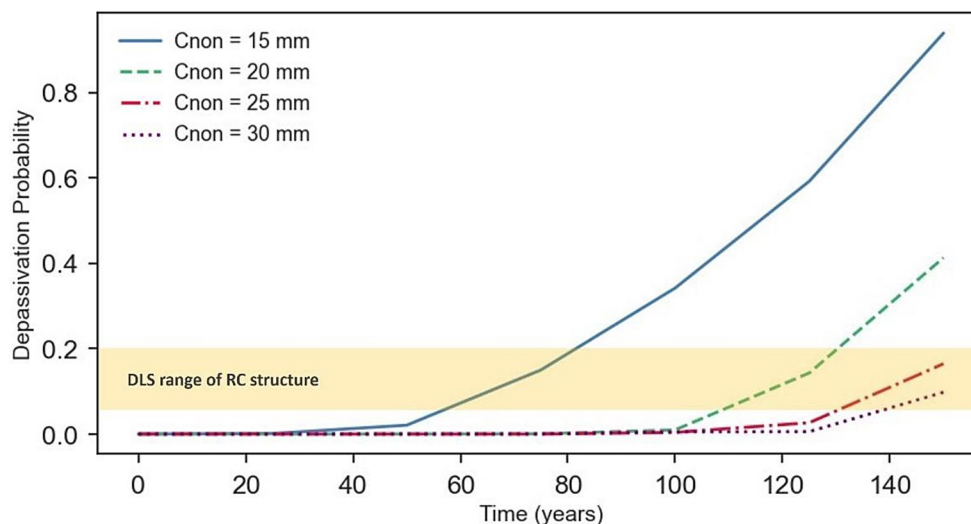
Fig. 17 Carbonation depth and cover thickness distributions for the Beam structure at (**a**) 50 years, (**b**) 75 years, (**c**) 125 years, and (**d**) 150 years

Fig. 18 Deterministic assessment of the design lives of RC structures

Fig. 19 Depassivation probability

4 Conclusions

This study introduces a probabilistic approach that utilizes artificial neural networks to accurately forecast the carbonation depth in reinforced concrete (RC) structures exposed to natural environments. The ANN model, which has been fine-tuned through extensive training and testing, shows a significant ability to apply learned knowledge to new situations. However, there are certain limits regarding the difference in performance between the training and test phases. Using a combined performance metric that balances R^2 and RMSE values from both phases, the [10-6-6-1] topology was identified as the most effective, achieving high coefficients of determination in the training and test phases, with values of 0.92 and 0.81, respectively.

An analysis of reinforced concrete structures demonstrates the real-world application of this theoretical framework. The probabilistic study, utilizing comprehensive climatic, structural, and material data, emphasizes the unpredictability and uncertainty inherent in durability estimates. The results indicate that, although the Brazilian codes provide a design life of 50 years, the assessed structures have demonstrated durability ranging from 109 to 139 years, depending on individual conditions and structural components.

The findings highlight the substantial disparity between deterministic and probabilistic assessments. Despite its simplicity, the deterministic analysis can greatly overstate the structure's durability, as indicated by disparities of up to 238% compared to probabilistic outcomes. This emphasizes the necessity of employing probabilistic methodologies in durability analysis to consider uncertainty in parameters and offer more dependable predictions.

Moreover, a parametric analysis reveals that the thickness of the concrete cover significantly impacts the durability of reinforced concrete structures. Decreasing the cover thickness from 20 mm to 15 mm results in an almost 50% reduction in design life, highlighting the crucial need for accurate implementation throughout construction.

Besides, the proposed probabilistic approach, augmented by ANN models, offers a comprehensive and reliable method for predicting the Likewise, the proposed probabilistic approach, enhanced by artificial neural network (ANN) models, provides a thorough and dependable technique for forecasting the degradation of reinforced concrete (RC) structures caused by carbonation. This methodology may substantially enhance the design and maintenance strategies, ensuring infrastructure's durability and safety.

Author contributions Conceptualization, E.F.F.; Data curation, B.M.L; T.L.G.T.B. and R.A.C.; Formal analysis, E.F.F. ,T.L.G.T.B. and R.A.C.; Funding acquisition, E.F.F.; Methodology, E.F.F.; B.M.L and R.A.C.; Project administration, E.F.F.; Software, B.M.L; T.L.G.T.B. and T.C.C.C; Supervision, E.F.F.; Writing—original draft, E.F.F., B.L.M.; Writing—review and editing, E.F.E.

Data availability No datasets were generated or analysed during the current study.

Declarations

References

1. Felix EF (2018) Modelagem Da Deformação do Concreto Armado Devido à Formação dos Produtos De Corrosão. University of São Paulo

2. Dal Molin D (1988) Fissuras em estruturas de concreto armado: análise das manifestações típicas e levantamento de casos ocorridos no estado do Rio Grande do sul. Universidade federal do Rio Grande do Sul

3. Carmen Andrade (1992) Manual para diagnóstico de obras deterioradas por corrosão de armaduras. PINI, São Paulo

4. Paulo Helene (1986) Corrosão em armaduras para concreto armado. PINI, São Paulo

5. Sanjuán MA, Andrade C, Cheyrezy M (2003) Concrete carbonation tests in natural and accelerated conditions. Adv Cem Res 15:171–180. https://doi.org/10.1680/adcr.2003.15.4.171

6. Possan E, Andrade JJO, Dal Molin DCC, Ribeiro JLD (2021) Model to Estimate Concrete Carbonation Depth and Service Life Prediction. pp 67–97

7. Kobayashi K, Uno Y (1990) Mechanism of carbonation of concrete. Concrete Libr JSCE 16:139–151

8. Venkat Rao N, Meena T (2017) A review on carbonation study in concrete. IOP Conf Ser Mater Sci Eng 263:032011. https://doi.org/10.1088/1757-899X/263/3/032011

9. Fuhaid AF, Al, Niaz A (2022) Carbonation and corrosion problems in Reinforced concrete structures. Buildings 12:586. https://doi.org/10.3390/buildings12050586

10. Huo Z, Wang L, Huang Y (2023) Predicting carbonation depth of concrete using a hybrid ensemble model. J Building Eng 76:107320. https://doi.org/10.1016/j.jobe.2023.107320

11. Rozière E, Loukili A, Cussigh F (2009) A performance based approach for durability of concrete exposed to carbonation. Constr Build Mater 23:190–199. https://doi.org/10.1016/j.conbuildmat.2008.01.006

12. Felix EF, Possan E, Carrazedo R (2021) Artificial Intelligence Applied in the Concrete Durability Study

13. Felix EF, Possan E, Carrazedo R (2019) Analysis of training parameters in the ANN learning process to mapping the concrete carbonation depth. J Building Pathol Rehabilitation 4. https://doi.org/10.1007/s41024-019-0054-8

14. Félix EF, Falcão I, da Santos S LG, et al (2023) A Monte Carlo-Based Approach to assess the reinforcement depassivation probability of RC structures: Simulation and Analysis. Buildings 13:993. https://doi.org/10.3390/buildings13040993

15. Papadakis VG, Vayenas CG, Fardis MN (1991) Fundamental modeling and experimental investigation of concrete carbonation. ACI Mater J 88. https://doi.org/10.14359/1863

16. Jiang L, Lin B, Cai Y (2000) A model for predicting carbonation of high-volume fly ash concrete. Cem Concr Res 30:699–702. https://doi.org/10.1016/S0008-8846(00)00227-1

17. Saetta AV, Vitaliani RV (2004) Experimental investigation and numerical modeling of carbonation process in reinforced concrete structures. Cem Concr Res 34:571–579. https://doi.org/10.1016/j.cemconres.2003.09.009

18. de Rincón OT, Montenegro JC, Vera R et al (2015) Concrete carbonation in Ibero-American Countries DURACON Project: six-year evaluation. CORROSION 71:546–555. https://doi.org/10.5006/1385

19. Felix EF, Carrazedo R (2021) Análise probabilística Da Vida útil De Lajes De Concreto Armado Sujeitas à corrosão Por carbonatação via simulação De Monte Carlo. Matéria (Rio De Janeiro) 26. https://doi.org/10.1590/s1517-707620210003.13043

20. Chang C-F, Chen J-W (2006) The experimental investigation of concrete carbonation depth. Cem Concr Res 36:1760–1767. https://doi.org/10.1016/j.cemconres.2004.07.025

21. Tuutti K (1982) Corrosion of Steel in Concrete. Stockholm

22. Lovato PS, Possan E, Molin DCCD et al (2012) Modeling of mechanical properties and durability of recycled aggregate concretes. Constr Build Mater. https://doi.org/10.1016/j.conbuildmat.2011.06.043. 26:

23. Ghanooni-Bagha M, YekeFallah MR, Shayanfar MA (2020) Durability of RC structures against Carbonation-Induced Corrosion under the impact of Climate Change. KSCE J Civ Eng 24:131–142. https://doi.org/10.1007/s12205-020-0793-8

24. Kari OP, Puttonen J, Skantz E (2014) Reactive transport modelling of long-term carbonation. Cem Concr Compos. https://doi.org/10.1016/j.cemconcomp.2014.05.003. 52:

25. Broomfield J (2006) Corrosion of Steel in concrete: understanding, Investigation and Repair, 2nd edn. CRC Press;, London

26. Köliö A, Pakkala TA, Hohti H et al (2017) The corrosion rate in reinforced concrete facades exposed to outdoor environment. Mater Struct 50. https://doi.org/10.1617/s11527-016-0920-7

27. Du X, Jin L (2014) Meso-scale numerical investigation on cracking of cover concrete induced by corrosion of reinforcing steel. Eng Fail Anal 39:21–33. https://doi.org/10.1016/j.engfailanal.2014.01.011

28. Felix EF, Carrazedo R, Possan E (2021) Carbonation model for fly ash concrete based on artificial neural network: development and parametric analysis. Constr Build Mater 266. https://doi.org/10.1016/j.conbuildmat.2020.121050

29. Silvestro L, Andrade JJO, Dal Molin DCC (2019) Evaluation of service-life prediction model for reinforced concrete structures in chloride-laden environments. J Building Pathol Rehabilitation 4:20. https://doi.org/10.1007/s41024-019-0059-3

30. Lee H, Lee H-S, Suraneni P (2020) Evaluation of carbonation progress using AIJ model, FEM analysis, and machine learning algorithms. Constr Build Mater 259:119703. https://doi.org/10.1016/j.conbuildmat.2020.119703

31. Silva A, Neves R, de Brito J (2014) Statistical modelling of carbonation in reinforced concrete. Cem Concr Compos 50:73–81. https://doi.org/10.1016/j.cemconcomp.2013.12.001

32. Kari OP, Puttonen J, Skantz E (2014) Reactive transport modelling of long-term carbonation. Cem Concr Compos 52:42–53. https://doi.org/10.1016/j.cemconcomp.2014.05.003

33. Chen Z, Lin J, Sagoe-Crentsil K, Duan W (2022) Development of hybrid machine learning-based carbonation models with weighting function. Constr Build Mater 321:126359. https://doi.org/10.1016/j.conbuildmat.2022.126359

34. Torres H, Correa E, Castaño JG, Echeverría F (2017) Simplified Mathematical Model for concrete carbonation. J Mater Civ Eng 29. https://doi.org/10.1061/(ASCE)MT.1943-5533.0002001

35. Trevisol CA, da Silva PRP, Paula MM, da Pelisser S F (2017) Avaliação De inibidores de corrosão para estruturas de concreto armado. Matéria (Rio De Janeiro) 22. https://doi.org/10.1590/s1517-707620170004.0238

36. Liberati EAP, Leonel ED, Nogueira CG (2014) Influence of the reinforcement corrosion on the bending moment capacity of reinforced concrete beams: a structural reliability approach. Revista IBRACON De Estruturas E Materiais 7:379–413. https://doi.org/10.1590/S1983-41952014000300005

37. Ramezanianpour AA, Tarighat A, Miyamoto A (2000) Concrete Carbonation Modelling and Monte Carlo Simulation Method for Uncertainty Analysis of Stochastic Front Depth. Mem Fac Eng Yamaguchi Univ 50

38. Aslani F, Dehestani M (2020) Probabilistic impacts of corrosion on structural failure and performance limits of reinforced concrete beams. Constr Build Mater 265:120316. https://doi.org/10.1016/j.conbuildmat.2020.120316

39. Kirkpatrick TJ, Weyers RE, Anderson-Cook CM, Sprinkel MM (2002) Probabilistic model for the chloride-induced corrosion service life of bridge decks. Cem Concr Res 32:1943–1960. https://doi.org/10.1016/S0008-8846(02)00905-5

40. Li Q, Li K, Zhou X et al (2015) Model-based durability design of concrete structures in Hong Kong–Zhuhai–Macau sea link project. Struct Saf 53:1–12. https://doi.org/10.1016/j.strusafe.2014.11.002

41. Saassouh B, Lounis Z (2012) Probabilistic modeling of chloride-induced corrosion in concrete structures using first- and second-order reliability methods. Cem Concr Compos 34:1082–1093. https://doi.org/10.1016/j.cemconcomp.2012.05.001

42. Al-alaily HS, Hassan A, Hussein AA AA (2017) Probabilistic and statistical modeling of Chloride-Induced corrosion for concrete containing metakaolin. J Mater Civ Eng 29. https://doi.org/10.1061/(ASCE)MT.1943-5533.0002062

43. Lizarazo-Marriaga J, Higuera C, Guzmán I, Fonseca L (2020) Probabilistic modeling to predict fly-ash concrete corrosion initiation. J Building Eng 30:101296. https://doi.org/10.1016/j.jobe.2020.101296

44. Pellizzer GP, Leonel ED (2020) Probabilistic corrosion time initiation modelling in reinforced concrete structures using the BEM. Revista IBRACON De Estruturas E Materiais 13. https://doi.org/10.1590/s1983-41952020000400009

45. Ann KY, Pack SW, Hwang JP et al (2010) Service life prediction of a concrete bridge structure subjected to carbonation. Constr Build Mater 24:1494–1501. https://doi.org/10.1016/j.conbuildmat.2010.01.023

46. Liang M-T, Huang R, Fang S-A (2013) Carbonation service life prediction of existing concrete viaduct/bridge using time-dependent analysis. J Mar Sci Technol 21

47. Yu B, Fang Z, Gao Y et al (2023) Carbonation of supersulfated cement concrete after 8 years of natural exposure. Cem Concr Compos 142. https://doi.org/10.1016/j.cemconcomp.2023.105165

48. Rathnarajan S, Dhanya BS, Pillai RG et al (2022) Carbonation model for concretes with fly ash, slag, and limestone calcined clay - using accelerated and five - year natural exposure data. Cem Concr Compos 126. https://doi.org/10.1016/j.cemconcomp.2021.104329

49. Liisma E, Sein S, Järvpõld M (2017) The influence of carbonation process on concrete bridges and durability in Estonian practice. IOP Conf Ser Mater Sci Eng 251. https://doi.org/10.1088/1757-899X/251/1/012072

50. Malysz GN, Bosse RM, De Miranda Saleme Gidrão G et al (2023) Service-life prediction of recycled coarse aggregate concrete under natural carbonation: a time-dependent reliability analysis. Constr Build Mater 387. https://doi.org/10.1016/j.conbuildmat.2023.131632

51. Ribeiro AB, Santos T, Gonçalves A (2018) Performance of concrete exposed to natural carbonation: use of the k-value concept. Constr Build Mater 175:360–370. https://doi.org/10.1016/j.conbuildmat.2018.04.206

52. Huy Vu Q, Pham G, Chonier A et al (2019) Impact of different climates on the resistance of concrete to natural carbonation. Constr Build Mater 216:450–467. https://doi.org/10.1016/j.conbuildmat.2019.04.263

53. De Melo SK, CARBONATAÇÃO NATURAL DE CONCRETOS COM ADIÇÕES MINERAIS AO LONGO DE 20 ANOS (2022) Retenção De água livre e o avanço da frente de carbonatação. Master, Universidade Federal de Goiás

54. Almeida TA, da Felix C, de Sousa EF CMA, et al (2023) Influence of the ANN Hyperparameters on the Forecast accuracy of RAC's compressive strength. Materials 16:7683. https://doi.org/10.3390/ma16247683

55. Ling H, Qian C, Kang W et al (2019) Combination of support Vector Machine and K-Fold Cross validation to predict compressive strength of concrete in marine environment. Constr Build Mater 206:355–363. https://doi.org/10.1016/j.conbuildmat.2019.02.071

56. Lyu Z, Yu Y, Samali B et al (2022) Back-propagation neural network optimized by K-Fold Cross-validation for Prediction of Torsional Strength of Reinforced concrete Beam. Materials 15:1477. https://doi.org/10.3390/ma15041477

57. Sechidis K, Tsoumakas G, Vlahavas I (2011) On the Stratification of Multi-label Data. pp 145–158

58. Krogh A (2008) What are artificial neural networks? Nat Biotechnol 26:195–197. https://doi.org/10.1038/nbt1386

59. Felix EF, Possan E, Carrazedo R (2021) A New Formulation to Estimate the Elastic Modulus of recycled concrete based on regression and ANN. Sustainability 13:8561. https://doi.org/10.3390/su13158561

60. Marek P, Guštar M, Tikalsky PJ (1993) Monte Carlo Simulation—Tool for Better understanding of LRFD. J Struct Eng 119:1586–1599. https://doi.org/10.1061/(ASCE)0733-9445(1993)119:5(1586)

61. Beck AT (2019) Confiabilidade E segurança Das Estruturas. Elsevier Brasil

62. Jacquemart D, Morio J, Le Gland F, Balesdent M (2016) Special developments for time-variant systems. Estimation of rare event probabilities in Complex Aerospace and Other Systems. Elsevier, pp 137–153

63. Possamai BB (2022) Processo de Cálculo para Análise Probabilística Estácionaria do Estado Limite de Durabilidade de Estruturas de Concreto Armado Sujeitas à Ação do Dióxido de Carbono. Bachelor Thesis, Universidade Federal da Integração Latino Americana

64. Possan E, Berwanger C, Rigo E et al (2020) Protection of interrupted concrete structure to prevent degradation: a case study. J Building Pathol Rehabilitation 5:18. https://doi.org/10.1007/s41024-020-00083-1

65. Enright MP, Frangopol DM (1998) Probabilistic analysis of resistance degradation of reinforced concrete bridge beams under corrosion. Eng Struct 20:960–971. https://doi.org/10.1016/S0141-0296(97)00190-9

66. Instituto Nacional de Meteorologia (BDMEP/INMET) (2022) Banco De Dados Meteorológicos para Ensino E Pesquisa. Temperaturas máximas e mínimas e humidade relativa do ar anos 2012/2022. In: Banco de Dados Meteorológicos para Ensino e Pesquisa

67. 2 Degrees Institute (2022) CO2 mudial concentration. In: CO2 levels Data Base

68. Associação Brasileira de Normas Técnicas (ABNT) (2013) NBR 15575-1: Edifícios Habitacionais - Desempenho: Parte 1 : Requisitos Gerais. Rio de janeiro

69. ISO T (2008) General principles on the design of structures for durability

70. Palm V, Maran AP, Barreto MFFM et al (2020) Influência Da distribuição De espaçadores no cobrimento e na vida útil de lajes maciças. Ambiente Construído 20:671–686. https://doi.org/10.1590/s1678-86212020000300452